

Accepted Manuscript

Rational design of mitochondria-targeted pyruvate dehydrogenase kinase 1 inhibitors with improved selectivity and antiproliferative activity

Biao Xu, Zhimei Yu, Sichuan Xiang, Yunshan Li, Shao-Lin Zhang, Yun He



PII: S0223-5234(18)30503-8

DOI: [10.1016/j.ejmech.2018.06.012](https://doi.org/10.1016/j.ejmech.2018.06.012)

Reference: EJMECH 10482

To appear in: *European Journal of Medicinal Chemistry*

Received Date: 11 April 2018

Revised Date: 31 May 2018

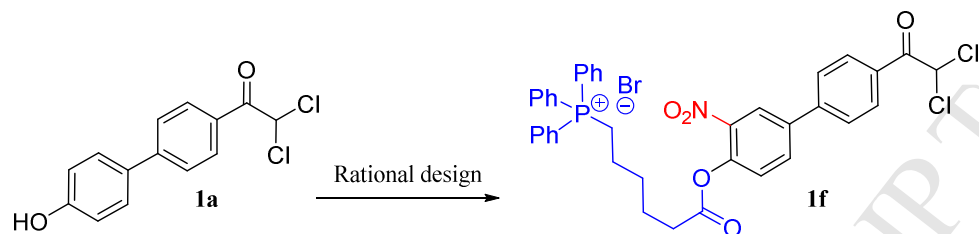
Accepted Date: 4 June 2018

Please cite this article as: B. Xu, Z. Yu, S. Xiang, Y. Li, S.-L. Zhang, Y. He, Rational design of mitochondria-targeted pyruvate dehydrogenase kinase 1 inhibitors with improved selectivity and antiproliferative activity, *European Journal of Medicinal Chemistry* (2018), doi: 10.1016/j.ejmech.2018.06.012.

This is a PDF file of an unedited manuscript that has been accepted for publication. As a service to our customers we are providing this early version of the manuscript. The manuscript will undergo copyediting, typesetting, and review of the resulting proof before it is published in its final form. Please note that during the production process errors may be discovered which could affect the content, and all legal disclaimers that apply to the journal pertain.

Graphical Abstract

With a rational design strategy, a triphenylphosphonium cation moiety and a nitro group were incorporated into **1a**, affording **1f** with improved target inhibition and selectivity.



Comp. ID	EC_{50} (μM)	IC_{50} (μM)		Selectivity index
		NCI-H1650 (cancer)	BEAS-2B (normal)	
1a	3.8	2.25	2.78	$2.78 / 2.25 = 1.2$
1f	0.1	0.21	3.28	$3.28 / 0.21 = 15.6$

Title page**Title:**

Rational design of mitochondria-targeted pyruvate dehydrogenase kinase 1 inhibitors with improved selectivity and antiproliferative activity

Author names and affiliations:

Biao Xu, Zhimei Yu, Sichuan Xiang, Yunshan Li, Shao-Lin Zhang,* Yun He*

School of Pharmaceutical Sciences, Chongqing Key Laboratory of Natural Product Synthesis and Drug Research, Chongqing University, Chongqing, 401331, P. R. China

* Corresponding address:

Dr. Shao-Lin Zhang & Prof. Dr. Yun He, School of Pharmaceutical Sciences, Chongqing Key Laboratory of Natural Product Synthesis and Drug Research, Chongqing University, Chongqing, 401331, P. R. China
Tel.: +86-23-65678465; E-mail: zhangsl@cqu.edu.cn; yun.he@cqu.edu.cn

Abstract:

Herein, triphenylphosphonium cation moieties were incorporated into a dichloroacetophenone derivative, leading to the discovery of novel mitochondria-targeted and tumor-specific pyruvate dehydrogenase kinase (PDK1) inhibitors. Biological studies suggested that all these synthesized compounds had significant *in vitro* activities, in particular compound **1f**, which inhibited PDK1 with an EC₅₀ value of 0.12 μM, and reduced the proliferation of NCI-H1650 cell with an IC₅₀ value of 0.21 μM, but showed marginal effect against non-cancerous BEAS-2B cell (IC₅₀ = 3.28 μM). In addition, **1f** decreased the extracellular acidification rate and lactate formation, increased reactive oxygen species production, and depolarized the mitochondrial membrane potential of NCI-H1650 cell, which could serve as a potential modulator to reactive mitochondrial oxidative phosphorylation and reprogram the glucose metabolic pathways in cancer cells. Collectively, these data demonstrated that **1f** could be a promising lead for the development of therapeutic PDK1 inhibitor in cancer treatment.

Keywords:

Cancer metabolism; Cancer proliferation; Mitochondria; Triphenylphosphonium cation; Anti-cancer drug

1. Introduction

Cancer cells exhibit an increased glycolysis and suppressed oxidative phosphorylation (OXPHOS), even under aerobic conditions [1, 2]. This metabolic alteration and adaptation is believed to provide proliferative advantages and survival needs for cancer cells [3]. Thus, selective disruption of the metabolic aberrations may offer therapeutic opportunities in cancer therapy [4].

Pyruvate dehydrogenase complex (PDC) is a gatekeeper enzyme, linking the glycolysis and tricarboxylic acid cycle, which regulates the flux of the pyruvate into mitochondria for OXPHOS [5]. The activity of PDC is regulated by the reversible phosphorylation. The phosphorylation of PDC by the four isoforms of PDK (PDK1, 2, 3 and 4) results in its inactivation, while the dephosphorylation by two pyruvate dehydrogenase phosphatases (PDPs) restores its activity [6, 7]. Therefore, inhibition of PDKs to activate PDC is an attractive therapeutic strategy to reverse the abnormal metabolic pathways and inhibit cancer cell proliferation.

Among the four PDK isoforms, PDK1 is most associated with cancer malignancy [8]. It had been reported that PDK1 was remarkably overexpressed in various human tumor samples, such as head and neck squamous cancer [9], gastric cancer [10] and lung cancer [11, 12]. Furthermore, overexpression of PDK1 protected cancer cells from anoikis, while depletion of the enzyme restored the susceptibility to anoikis and reduced the metastatic potential [13]. In addition, a recent study indicated that PDK1 activity was increased at the post-transcriptional level by diverse oncogenic tyrosine kinases [14]. This enhancement of PDK1 activity resulted in a promotion of the Warburg effect and tumor growth [15]. Collectively, these studies suggested that PDK1 was an attractive target. Inhibition of PDK1 could provide a promising approach to kill or, at least, greatly reduce the growth of cancer cells.

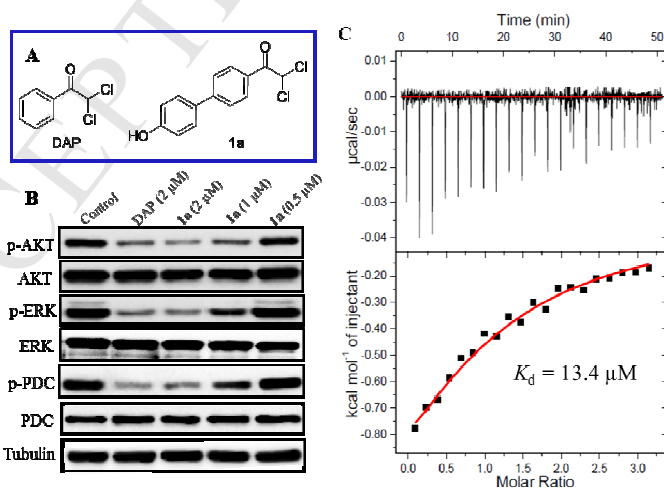


Fig. 1 Biological activities of DAP and 1a. A: Chemical structures of DAP and 1a. B: DAP and 1a at different concentrations inhibited proteins phosphorylation in AKT, ERK and PDC signaling pathways. C: 1a bound to PDK1 protein with a K_d value of 13.4 μM .

Recently, several inhibitors have been reported to inhibit the activity of PDKs and reduced cancer cells proliferation [16–18]. Dichloroacetophenone (DAP, **Fig. 1A**) was identified as a PDKs inhibitor in a screening campaign based on pyruvate dehydrogenase activity [19], which was never used in anticancer studies. Until recently, Qin *et al* reported that DAP weakly inhibited the acute myeloid leukemia (AML) cells proliferation [20]. However, DAP is not a specific PDKs inhibitor, which affects other signal pathways, such as AKT and ERK phosphorylations (**Fig. 1B**), therefore inevitably leading to some off-target and / or side effects. Continuing our endeavor to discover specific PDK1 inhibitor [21, 22], we identified a structurally novel PDK1 inhibitor **1a**, which dose-dependently inhibited PDC phosphorylation (**Fig. 1B**) and bound to PDK1 protein with a K_d value of 13.4 μM (**Fig. 1C**). Unfortunately, **1a** affected ERK and AKT signaling pathways, similar to DAP, and therefore resulted in no selectivity. Inspired by these preliminary results, we herein report the rational design and identification of a series of novel mitochondria-targeted and tumor-specific PDK1 inhibitors with reduced off-target and / or side effects as compared to their parent molecule.

2. Results and discussion

2.1. Design strategy of TPP⁺-conjugated compounds

One of the major challenges in developing anticancer drugs is to improve selectivity and reduce side effects for normal cells. As we stated above, the PDK1 inhibitor **1a** affected the ERK and AKT protein phosphorylation, which could inevitably result in undesired side effects. As expected, comparisons of the IC_{50} values between tumor cell line NCI-H1650 ($\text{IC}_{50} = 2.25 \mu\text{M}$) and non-cancerous cell BEAS-2B ($\text{IC}_{50} = 2.78 \mu\text{M}$) indicated that **1a** displayed almost the same cytotoxicity between the two cell lines. To the best of our knowledge, the ERK and AKT proteins mainly locate in cytoplasm, while PDKs exist mainly in mitochondria. We hypothesize that if we specifically transport a PDKs inhibitor into cancer cell mitochondria, it would avoid disrupting the ERK and AKT signal pathway.

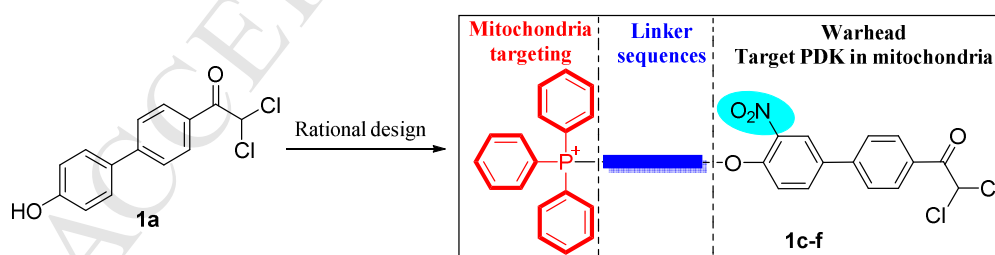


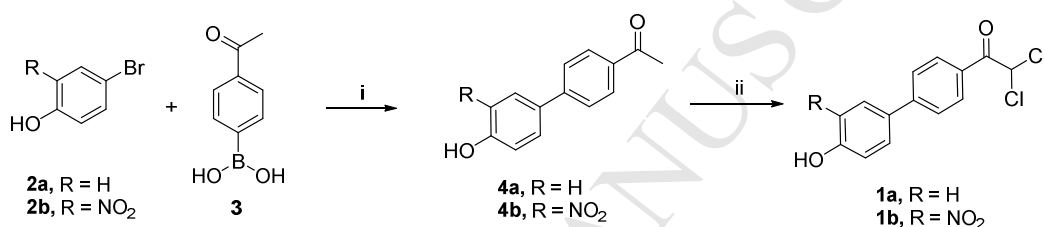
Fig. 2 Design of TPP⁺-conjugated compounds

Generally, most cancer cells exhibit an elevated mitochondrial membrane potential ($\Delta\psi\text{m}$) at least 60 mV as compared to normal cells, which could be exploited to selectively target mitochondria for cancer therapy [23]. Triphenylphosphonium cation (TPP⁺) is widely used as a mitochondria-targeted moiety, and the utilizing of TPP⁺ as a mitochondria-targeted vehicle has been well studied [24]. With this notion in our

mind, we tethered triphenylphosphonium cations (TPP^+) to a PDK1 inhibitor, with the aim to generate specific mitochondria-targeted compounds to avoid off-target and / or side effects. As shown in **Fig. 2**, the warhead is a parent molecule that inhibits PDK1 function and cancer cell proliferation. The end of the warhead is attached to a TPP^+ moiety through alkyl linkers, which were expected to modulate the lipophilicity and cellular uptake of the target compounds.

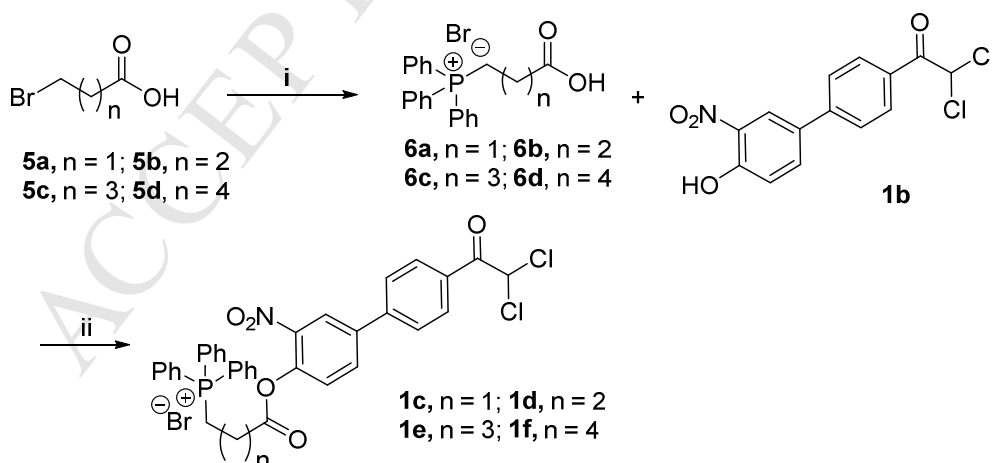
2.2. Synthesis of TPP^+ -conjugated compounds

The preparation of the TPP^+ -conjugated compounds were shown in **Schemes 1** and **2**. The reaction of arylhalides (**2a** and **2b**) with 4-acetyl-phenylboronic acid (**3**) yielded compounds **4a** and **4b**, which were chlorinated in the presence of copper(II) chloride dehydrate and lithium chloride to conveniently produce dichloro-substituted compounds **1a** and **1b**.



Scheme 1 Synthetic routes of the parent molecules **1a** and **1b**. Reagents and conditions: (i) K_2CO_3 , H_2O , $(n\text{-Bu})_4\text{NBr}$, $\text{Pd}(\text{OAc})_2$, $70\text{ }^\circ\text{C}$; (ii) $\text{CuCl}_2 \cdot 2\text{H}_2\text{O}$, LiCl , DMF , $90\text{ }^\circ\text{C}$.

The brominated carboxylic acids (**5a–d**) were then stirred with triphenyl phosphines in dry acetonitrile to afford the phosphates (**6a–d**) with yields ranging from 87 to 95%. Finally, **1b** and phosphates (**6a–d**) coupled efficiently and gave the TPP^+ -conjugated compounds **1c–f**. All these target compounds **1a–f** were characterized by ^1H NMR, ^{13}C NMR and HRMS spectra (Supporting information).



Scheme 2 Synthetic routes of the TPP^+ -conjugated target compounds **1c–f**. Reagents and conditions: (i) $\text{P}(\text{Ph})_3$, dry CH_3CN , reflux; (ii) DCC , anhydrous DCM , RT .

2.3. TPP⁺-conjugated compounds have little effect on the ERK and AKT signaling pathways

We aimed to develop PDK-selective anticancer compounds by minimizing their activities on AKT and ERK signal pathways. Therefore, the target compounds first were chosen to assess their effect on AKT and ERK phosphorylation through Western blotting experiments. As shown in **Fig. 3**, DAP, **1a** and **1b** at 2 μ M strongly reduced the AKT and ERK phosphorylation. Interestingly, the TPP⁺-conjugated compounds **1c–f** displayed a minimal effect on AKT and ERK phosphorylation, which was in full agreement with our hypothesis.

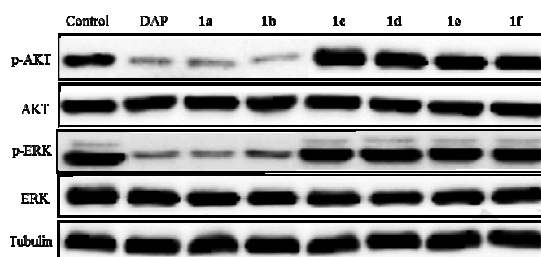


Fig. 3 Proteins phosphorylation in AKT and ERK signaling pathways after treated with DAP (2 μ M) and **1a–1f** (2 μ M) in NCI-H1650 cells for 12 h.

2.4. TPP⁺-conjugated compounds inhibit cancer cell proliferation and PDKs activity

With the improved selectivity of TPP⁺-conjugated compounds, next the growth inhibitory effects of DAP, **1a–f**, and **6a–d** against the cancer cell lines MCF-7, A375 and NCI-H1650 were then measured. A non-cancerous BEAS-2B cell was included to compare the selectivity of these compounds. Exposure of the cells to the compounds for 72 h resulted in dose-dependent decreases in cell viability, except for compounds **6a–d**, which could rule out the possibility that the observed cytotoxicity is due to the TPP⁺ moieties. As shown in Table 1, **1a** exhibited strong antiproliferative activities against MCF-7, A375 and NCI-H1650 cells, but its ability to inhibit PDKs (primary dehydrogenase enzymatic assay) was weak, with an EC₅₀ value of 3.8 μ M, suggesting that **1a** is not a specific PDKs inhibitor. Based on our previous study (data are not shown here), the nitro-substitution in meta-position of benzene ring was beneficial for inhibiting PDKs function, so a nitro group was introduced into **1a**. As expected, the designed compound **1b** displayed an improved PDKs inhibitory potency with the EC₅₀ value of 0.25 μ M, however, the selective-index (SI) value for **1b** is only 1.6, as shown in Table 1. The introduction of TPP⁺ moieties offered the TPP⁺-conjugated compounds **1c–f**, which strongly inhibited cancer proliferation and PDKs function. Interestingly, the SI values of **1c–f** were also greatly increased, indicating that the TPP⁺-conjugated compounds selectively inhibit cancer cells, but not non-cancerous cells. Of note, compound **1f** with a linker of six carbon atoms displayed a potent growth inhibitory effect on NCI-H1650 cell (Fig. S1 in Supporting Information), the IC₅₀ value is 0.21 μ M. Compound **1f** also exhibited promising

PDKs inhibitory potency ($EC_{50} = 0.1 \mu\text{M}$), which warranted for further investigation.

Table 1 Biological evaluation of compounds **1a–f**, **6a–d** and DAP.

Cpds.	IC_{50} (μM)					PDKs inhibition (EC_{50} , μM)
	MCF-7	A375	NCI-H1650	BEAS-2B ^a	SI ^b	
1a	1.38 ± 0.22	1.1 ± 0.25	2.25 ± 0.30	2.78 ± 0.32	1.2	3.80 ± 1.41
1b	0.63 ± 0.11	0.75 ± 0.19	0.92 ± 0.27	1.44 ± 0.10	1.6	0.25 ± 0.09
1c	1.78 ± 0.30	1.38 ± 0.21	0.87 ± 0.14	6.5 ± 0.92	7.5	0.34 ± 0.10
1d	0.97 ± 0.12	1.27 ± 0.30	0.85 ± 0.14	> 10	> 10	0.36 ± 0.04
1e	0.81 ± 0.17	1.18 ± 0.21	0.88 ± 0.15	4.82 ± 0.10	5.5	0.14 ± 0.02
1f	0.50 ± 0.11	0.51 ± 0.09	0.21 ± 0.04	3.28 ± 0.08	15.6	0.10 ± 0.02
6a	NI	NI	NI	NI ^c		NT ^d
6b	NI	NI	NI	NI		NT
6c	NI	NI	NI	NI		NT
6d	NI	NI	NI	NI		NT
DAP	12.5 ± 2.1	8.5 ± 1.2	6.8 ± 0.91	7.7 ± 1.5	1.1	NI

^a A normal human epithelial cells isolated from bronchial epithelium; ^b Selective-index is calculated by comparing the IC_{50} values in human normal BEAS-2B cells against the IC_{50} value of the same compound in NCI-H1650 cancer cells; ^c NI represents no inhibition; ^d NT represents not tested.

To explore the mechanism of cancer cells death, DAP and **1f** were used to induce NCI-H1650 cells apoptosis, which was then examined with the Annexin V-FITC/PI FACS assay. As shown in **Fig. 4**, the percentages of apoptotic population in NCI-H1650 cells treated with DAP at 10 μM for 12 h was 10.6%, while for **1f** at 0.5, 1 and 2 μM , the percentages were 7.2, 13.8, and 17.2%, respectively, clearly outperformed DAP in inducing cancer cell apoptosis. Moreover, the percentages of apoptosis for NCI-H1650 cells treated with **1f** at 1 μM for 6, 12 and 24 h were 6.6, 13.6, and 23.6 %, respectively, suggesting the induction of apoptosis by **1f** followed a time-dependent manner.

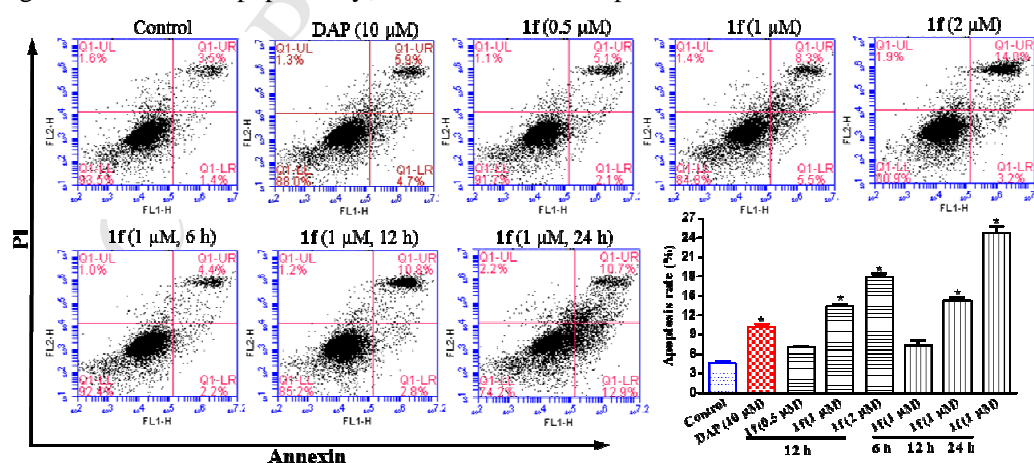


Fig. 4 Flow cytometer analysis of NCI-H1650 cells apoptosis. The cells were treated with DAP and **1f** for 6, 12 and 24 hours, then were stained with FITC Annexin V / PI. Cells in the upper right quadrant indicate PI positive/Annexin V positive, late

apoptotic, or necrotic cells, and cells in lower right quadrant indicate early apoptotic cells. Bar graph represents statistics of total apoptotic cell percentages from duplicate experiments. * $P < 0.05$, versus control group.

2.5. TPP⁺-conjugated compounds activate purified PDC by inhibiting PDK1

Compounds **1c–f** were next evaluated for their effects on PDC activation by a primary dehydrogenase enzymatic assay. As shown in **Fig. 5A**, the TPP⁺-conjugated compounds **1c–f** dramatically increased PDC activity. To confirm the activation of PDC were indeed caused by direct inhibition of PDKs, we terminated the kinase reaction with 55 mM of pyruvate and ADP before **1c–f** addition. We then observed that NADH formation was barely affected by the compounds (**Fig. 5B**), indicating that **1c–f** had no effect on the dehydrogenase activity. Clearly, the enhanced PDC activity was resulted from PDKs inhibition by the compounds. The PDK1 kinase inhibitory activity was further evaluated in the presence of **1f** *via* measuring ATP consumption by the enzyme. As shown in **Fig. 5C**, **1f** dose-dependently reduced PDK1 activity, with the EC₅₀ value of 0.12 μM. To verify that PDK1 inhibition would lead to the reduction of the PDC phosphorylation level in cancer cells, NCI-H1650 cells were treated with DAP, **1b**, and **1f** for 12 h, then PDC phosphorylation was analyzed by Western blotting experiment. As shown in **Fig. 5D**, **1f** dramatically reduced PDC phosphorylation level in a dose-responsive manner, while DAP and **1b** had no effect at the same concentrations.

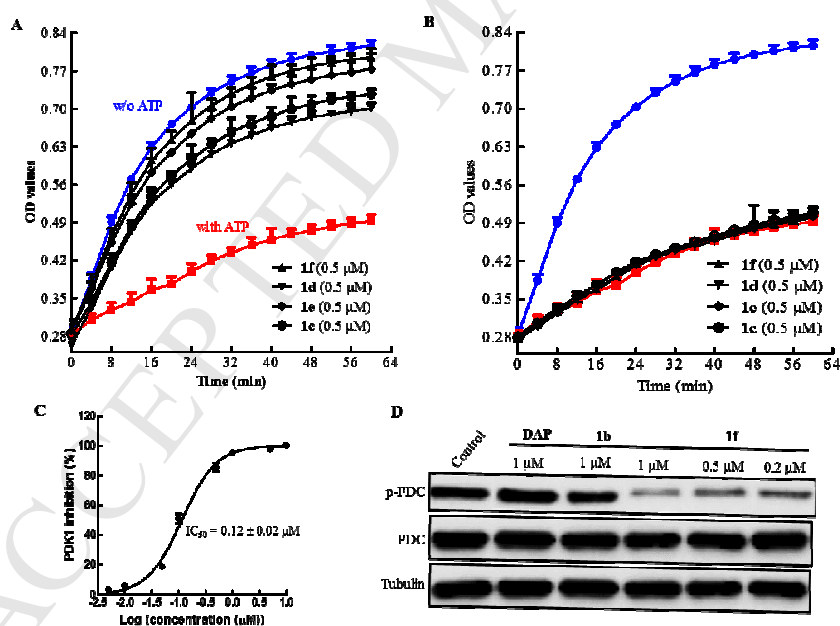


Fig. 5 Compound **1f** inhibited PDK1, and activated PDC activities. A: Compounds **1c–f** effect on PDC kinetics. OD_{340 nm} values were read at 37 °C. 'w/o ATP' represents maximal PDC activity when ATP was not included, while 'with ATP' represents minimal enzyme activity in the presence of 100 μM ATP. B: PDKs was inactivated, and then compounds **1c–f** effect on PDC kinetics. We run our experiments as singlet, but every dose was triplicate. The data was reported as Mean ± SD. C: Effect of **1f** on PDK1 kinase activity. D: Compounds **1f** exhibited dose response manner to inhibit PDC phosphorylation in NCI-H1650 cell, DAP and **1b** were used as control groups.

2.6. TPP⁺-conjugated compounds affect the mitochondrial bioenergetics function in NCI-H1650 cell

Inhibition of PDKs activates PDC, leading to a switch of pyruvate metabolism from lactate production to OXPHOS in mitochondria. Thus, the oxygen consumption and the degree of acidification will change in cancer cells. To explore whether TPP⁺-conjugated compounds confer this switching, NCI-H1650 cells were treated with **1b** (5 μ M), and **1f** (1, 2, and 5 μ M) for 4 h, then the changes in the extracellular acidification rates (ECAR) and oxygen consumption rates (OCR) were monitored on a Seahorse XFe24 extracellular flux, the lactate production was measured by a Nova Bioprofile Flex analyzer. As shown in **Fig. 6A** and **6B**, ECAR was significantly decreased with the addition of **1f**. As expected, OCR was increased. The enhancement of OCR for **1b** at 5 μ M is less significant than that of **1f** at the same concentration. We observed that **1f** at 2 or 5 μ M strongly inhibited the lactate formation in NCI-H1650 cell, clearly outperforming **1b** at 5 μ M (**Fig. 6C**). In addition, we measured the reactive oxygen species (ROS) production in NCI-H1650 cell treated with **1b** and **1f**. More ROS was generated with higher concentrations of **1f**, indicating an enhanced cellular respiration activity by the treatment of **1f** (**Fig. 6D**). Based on these results, we conclude that **1f** could elicit a metabolic alteration in cancer cells to enhance oxidative phosphorylation and ROS production, which might contribute to their anti-proliferation effect in the tumor cells.

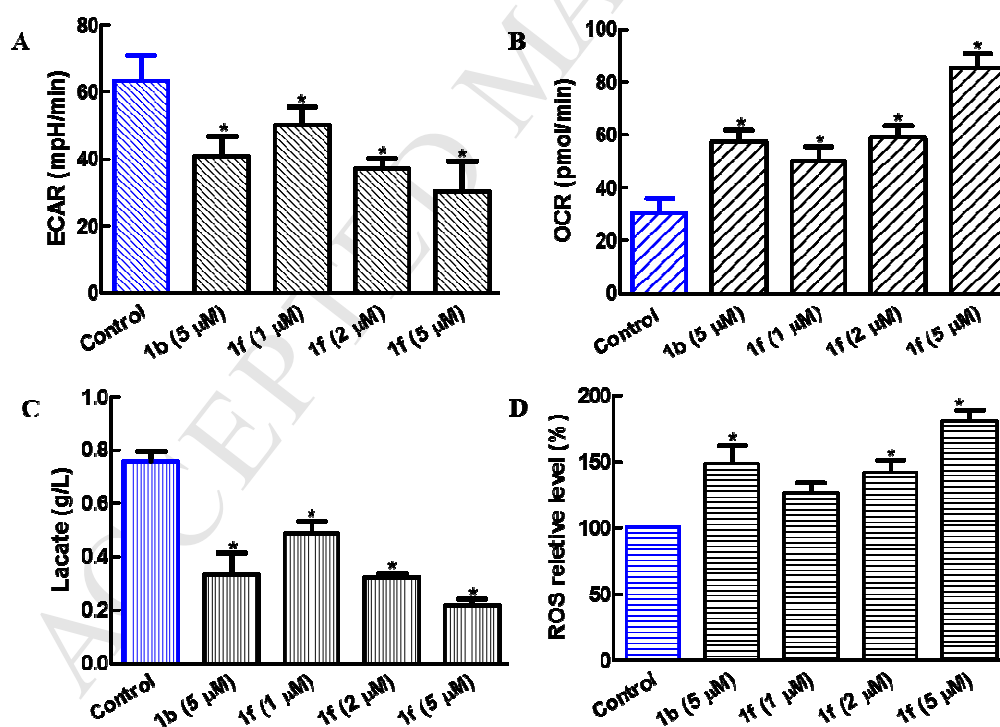


Fig. 6 Effect of **1b** and **1f** on mitochondrial bioenergetic function of NCI-H1650 cell. (A) ECAR was decreased by **1b** and **1f** treatment. (B) OCR was increased with the treatment of **1b** and **1f**. (C) Lactate formation was decreased by treatment of **1b** and **1f**. (D) ROS production was increased by treatment of **1b** and **1f**. * $P < 0.05$, versus the control group.

2.7. TPP⁺-conjugated compounds depolarize mitochondrial membrane potential in NCI-H1650 cells

Cancer cells exhibit hyperpolarized mitochondrial membrane potentials ($\Delta\psi_m$) as compared to normal cells. Depolarization of $\Delta\psi_m$ represents an effective strategy to inhibit cancer cell growth. Inhibitors targeting PDKs enhance the OXPHOS in cancer cell, and the $\Delta\psi_m$ should be decreased accordingly. To validate this hypothesis, NCI-H1650 cells were treated with **1b** (5 μ M) and **1f** (1, 2, and 5 μ M) for 4 hours, which were then stained with 5,5',6,6'-tetrachloro-1,1',3,3'-tetraethylbenzimidazolyl- carbocyanine iodide (JC-1), a cationic dye, which accumulated in mitochondria of high potential and was accompanied by a fluorescence emission shift from green to red due to the formation of the red fluorescent J-aggregates. Mitochondrial depolarization is indicated by an increased ratio of the green / red fluorescence intensity, which could be measured by a flow cytometer. As shown in **Fig. 8**, the quantitative analysis of JC-1 stained cells revealed a significant increase in the green (low $\Delta\psi_m$) / red (high $\Delta\psi_m$) ratio as compared to the cells treated with **1b** at 5 μ M or the control group, which suggested that **1f** depolarized the mitochondrial hyperpolarization and thus revived oxidative metabolism in cancer cells.

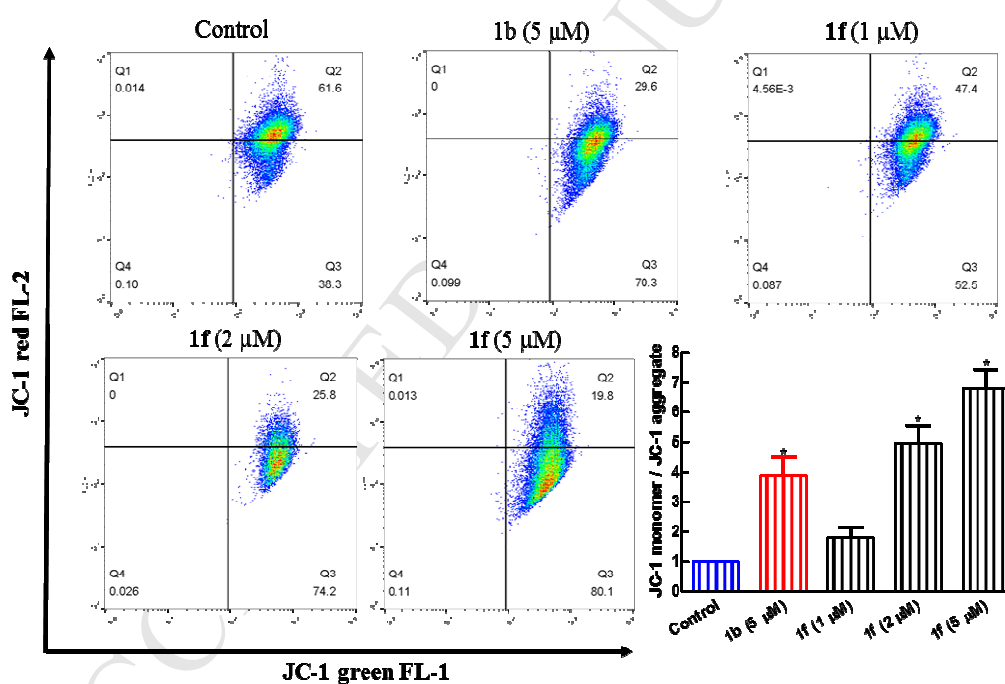


Fig. 7 Changes of $\Delta\psi_m$ in NCI-H1650 cells measured by JC-1 flow cytometry assay. Treatment of NCI-H1650 cells with **1b** (5 μ M), and **1f** (1, 2, and 5 μ M) for 4 h led to the decrease of $\Delta\psi_m$ in NCI-H1650 cells. The green FL-1 represents depolarized mitochondria (J-monomer), and the red FL-2 represents the hyperpolarized mitochondria (J-aggregates). The depolarization of $\Delta\psi_m$ is indicated by the increase in the ratio of J monomer/J aggregate. * $P < 0.05$, versus the control group.

3. Conclusion

We have developed novel TPP⁺-conjugated PDK1 inhibitors with improved potency and selectivity. The TPP⁺-conjugated compounds have abilities to enhance PDC enzymatic activity and PDK1 kinase inhibition. The MTT assay suggested that TPP⁺-conjugated compounds possessed prominent antiproliferative activities against NCI-H1650 cells with IC₅₀ values of 0.87, 0.85, 0.88 and 0.21 μM, respectively, while exhibiting little effect on the non-cancerous BEAS-2B cells. Meanwhile, the most potent **1f** among these compounds could alter the glucose metabolic profile in NCI-H1650 cells by decreasing ECRA and lactate formation, and increasing OCR values as well as ROS production. At last, **1f** was found to depolarize Δψ_m in NCI-H1650 cancer cells, which could trigger apoptotic stimuli and lead to cancer cell death. Collectively, our data demonstrated that TPP⁺-conjugated compounds, especially **1f** could be a promising lead for the developing therapeutic PDK1 inhibitor for cancer therapy.

4. Experimental protocols

4.1. General methods and target compounds synthesis

All chemicals were purchased from commercial source and used without further purification unless otherwise stated. The reactions were monitored by thin-layer chromatography and carried out on commercial Merck Kieselgel 60 F₂₅₄ plates, which could be visualized under UV light at 254 nm. Column chromatography was performed on silica gel. ¹H NMR spectra were obtained on an Agilent 400 MR spectrometer, while ¹³C NMR spectra were obtained with proton decoupling on an Agilent 400 MR DD2 (100 MHz) or 600 MR DD2 spectrometer and were reported in ppm with residual solvent for internal standard [δ 77.16 (CDCl₃)]. The chemical shifts were reported in parts per million (ppm), the coupling constants (J) were expressed in hertz (Hz) and signals were described as singlet (s), doublet (d), triplet (t), as well as multiplet (m). The NMR data was analyzed by MestReNova software. High-resolution mass spectra were obtained on a Bruker Solarix 7.0 T spectrometer. Melting points were recorded on a WRS-2A digital melting point apparatus. All other chemicals and solvents were commercially available, and were used as received.

4.1.1 Synthesis of compounds **4a–b**

To a round-bottom flask, 4.0 mmol of arylhalides (**2a** or **2b**), 4.4 mmol of 1-(4-acetyl-phenyl)-boronic acid (**3**), 0.2 mol % of Pd(OAc)₂, 10.0 mmol of powdered K₂CO₃ and 4.0 mmol of (*n*-Bu)₄NBr were added. The flask was flushed with nitrogen, water (4.4 mL) was added and the resulting suspension was stirred and heated for 4 h at 70 °C. After completion of the reaction, the mixture was diluted with water, and extracted with EtOAc (2 x 30 mL). The combined organic layers were dried over Na₂SO₄, filtered and concentrated. The crude residues were purified by silica gel chromatography to afford the pure compound (**4a** in 89 % yield, and **4b** in 83 %) [25].

1-(4'-Hydroxy-3'-nitro-[1,1'-biphenyl]-4-yl)ethan-1-one (4b). Compound **4b** was obtained as a yellow solid after the flash chromatography. M.p. 117–119 °C; ¹H NMR (400 MHz, CDCl₃): δ (ppm) 10.62 (s, 1H), 8.36–8.37 (m, 1H), 8.04–8.06 (m, 2H), 7.86–7.88 (m, 1H), 7.65–7.67 (m, 2H), 7.27–7.29 (m, 1H), 2.65 (s, 1H); ¹³C NMR (101 MHz, CDCl₃): δ (ppm) 197.35, 154.89, 142.54, 136.35, 136.10, 133.81, 132.39, 129.15, 126.73, 123.15, 120.73, 26.63; MS (ESI): m/z, 256.0 [M-H]⁺.

4.1.2 Synthesis of compounds **1a–b**

To a round-bottom flask 9.0 mmol of copper(II) chloride dihydrate, 9.0 mmol of lithium chloride and 1.5 mmol of the ketones (**4a** or **4b**) were added. Then DMF (7.0 mL) was added, the mixture was heated to 90 °C, and stirred for 6 h. Then the mixture was cooled to room temperature, diluted with water and extracted with ether (3 x 30 mL). The combined organic layers were washed with water (3 x 20 mL) and dried over Na₂SO₄, filtered and concentrated. The crude residues were purified by silica gel chromatography to afford the pure compounds.

2,2-Dichloro-1-(4'-hydroxy-[1,1'-biphenyl]-4-yl)ethan-1-one (1a). Compound **1a** was obtained as a yellow solid after flash chromatography. Yield: 48%; M.p. 114–117 °C; ¹H NMR (400 MHz, CDCl₃): δ (ppm) 8.13 (m, 2H), 7.67 (m, 2H), 7.54 (m, 2H), 6.93 (m, 2H), 6.68 (s, 1H); ¹³C NMR (101 MHz, CDCl₃): δ (ppm) 185.67, 156.71, 146.93, 131.55, 130.39, 129.17, 128.66, 126.76, 116.03, 67.82; MS (ESI): m/z, 279.0 [M-H]⁺; HRMS (ESI): calcd. for C₁₄H₉Cl₂O₂ [M-H]⁺: 278.9985, found: 278.9986.

2,2-Dichloro-1-(4'-hydroxy-3'-nitro-[1,1'-biphenyl]-4-yl)ethan-1-one (1b). Compound **1b** was obtained as a yellow solid after flash chromatography. Yield: 64%; M.p. 90–93 °C; ¹H NMR (400 MHz, CDCl₃): δ (ppm) 10.66 (s, 1H), 8.41 (s, 1H), 8.20–8.22 (m, 2H), 7.88–7.90 (m, 1H), 7.71–7.73 (m, 2H), 7.30–7.32 (m, 1H), 6.67 (s, 1H); ¹³C NMR (101 MHz, CDCl₃): δ (ppm) 185.29, 155.17, 143.96, 136.05, 133.85, 131.83, 130.67, 130.42, 126.96, 123.35, 120.93, 67.87; MS (ESI): m/z, 324.0 [M-H]⁺; HRMS (ESI): calcd. for C₁₄H₈Cl₂NO₄ [M-H]⁺: 323.9836, found: 323.9834.

4.1.3 Synthesis of compounds **1c–f**

To a round-bottom flask was added **5a** (5.0 mmol), P(Ph)₃ (20.0 mmol) and dry MeCN (10.0 mL). The mixture was stirred vigorously and heated to reflux. After the refluxing was ceased (15 h), the solution was concentrated. The residue was rinsed consecutively with benzene (3 x 10 mL), hexanes (10 mL), and ether (2 x 10 mL). The crystalline white solid was dried to give **6a** (1.8 g, 87%) [26]. **6b–d** were prepared in according to the procedure described as **6a**.

To a round-bottom flask was added **1b** (0.25 mmol), **6a** (0.2 mmol) and DCC (0.246 mmol). The flask was flushed with nitrogen, and then anhydrous DCM (6 mL) was added. The reaction was stirred at room temperature for one day. Then was filtered and concentrated, and purified by silica gel chromatography to afford compound **1c** in 70% yield [27]. Compounds **1d–f** were prepared in according to the procedure

described as **1c**.

(3-((4'-(2,2-Dichloroacetyl)-3-nitro-[1,1'-biphenyl]-4-yl)oxy)-3-oxopropyl)triphenylphosphonium bromide (**1c**). Compound **1c** was obtained as a white solid after flash chromatography. M.p. 89–93 °C; ¹H NMR (400 MHz, CDCl₃): (ppm) 8.27-8.28 (m, 1H), 8.21-8.23 (m, 2H), 7.82-7.93 (m, 10H), 7.69-7.76 (m, 9H), 6.67 (s, 1H), 4.41-4.47 (m, 2H), 3.31-3.37 (m, 2H); ¹³C NMR (101 MHz, CDCl₃): δ (ppm) 185.37, 161.04, 143.94, 143.58, 141.39, 138.47, 135.33, 133.73 (d, *J* = 10.1 Hz), 133.55, 130.67 (d, *J* = 12.1 Hz), 130.55, 130.42, 127.51, 127.26, 124.01, 117.61 (d, *J* = 86.9 Hz), 67.91, 27.62, 18.44 (d, *J* = 58.6 Hz); MS (ESI): *m/z*, 642.1 [M-Br]⁺; HRMS (ESI): calcd. for C₃₅H₂₇Cl₂NO₅P [M-Br]⁺: 642.0998, found: 642.1027.

(4-((4'-(2,2-Dichloroacetyl)-3-nitro-[1,1'-biphenyl]-4-yl)oxy)-4-oxobutyl)triphenylphosphonium (**1d**). Compound **1d** was obtained as a white solid after the flash chromatography. M.p. 117-120 °C; ¹H NMR (400 MHz, CDCl₃): (ppm) 8.32 (m, 1H), 8.21-8.24 (m, 2H), 7.86-7.92 (m, 7H), 7.78-7.80 (m, 3H), 7.65-7.75 (m, 9H), 6.68 (s, 1H), 4.15-4.23 (m, 2H), 3.37-3.40 (m, 2H), 2.09 (m, 2H); ¹³C NMR (101 MHz, CDCl₃): δ (ppm) 185.36, 171.18, 144.02, 143.62, 141.74, 138.30, 135.06, 133.68 (d, *J* = 10.1 Hz), 133.66, 130.90, 130.74, 130.51 (d, *J* = 13.1 Hz), 127.51, 126.76, 124.17, 118.01 (d, *J* = 86.9 Hz), 67.91, 33.31 (d, *J* = 19.2 Hz), 21.47 (d, *J* = 51.5 Hz), 17.80; MS (ESI): *m/z*, 656.1 [M-Br]⁺; HRMS (ESI): calcd. for C₃₆H₂₉Cl₂NO₅P [M-Br]⁺: 656.1155, found: 656.1155.

(5-((4'-(2,2-Dichloroacetyl)-3-nitro-[1,1'-biphenyl]-4-yl)oxy)-5-oxopentyl)triphenylphosphonium (**1e**). Compound **1e** was obtained as a white solid after the flash chromatography. M.p. 100–104 °C; ¹H NMR (400 MHz, CDCl₃): (ppm) 8.31 (m, 1H), 8.22-8.24 (m, 2H), 7.86-7.92 (m, 7H), 7.69-7.80 (m, 11H), 7.43-7.45 (m, 1H), 6.68 (s, 1H), 3.99-4.02 (m, 2H), 2.86-2.89 (m, 2H), 2.22-2.26 (m, 2H), 1.86-1.88 (m, 2H); ¹³C NMR (101 MHz, CDCl₃): δ (ppm) 185.42, 170.65, 143.78, 143.21, 141.64, 138.03, 134.96, 134.93, 133.50 (d, *J* = 10.1 Hz), 133.45, 130.95, 130.60, 130.39 (d, *J* = 13.1 Hz), 127.32, 126.15, 123.95, 117.92 (d, *J* = 85.9 Hz), 68.03, 32.87, 24.78 (d, *J* = 18.2 Hz), 22.36 (d, *J* = 69.7 Hz), 21.50; MS (ESI): *m/z*, 670.1 [M-Br]⁺; HRMS (ESI): calcd. for C₃₇H₃₁Cl₂NO₅P [M-Br]⁺: 670.1311, found: 670.1311.

(6-((4'-(2,2-Dichloroacetyl)-3-nitro-[1,1'-biphenyl]-4-yl)oxy)-6-oxohexyl)triphenylphosphonium (**1f**). Compound **1f** was obtained as a white solid after the flash chromatography. M.p. 94–97 °C; ¹H NMR (400 MHz, CDCl₃): (ppm) 8.31 (m, 1H), 8.21-8.23 (m, 2H), 7.86-7.95 (m, 7H), 7.68-7.81 (m, 11H), 7.49-7.51 (m, 1H), 6.69 (s, 1H), 3.91-3.98 (m, 2H), 2.67-2.71 (m, 2H), 1.80-1.89 (m, 4H), 1.69-1.75 (m, 2H); ¹³C NMR (101 MHz, CDCl₃): δ (ppm) 185.41, 170.98, 144.05, 143.53, 141.91, 138.10, 135.00, 133.63 (d, *J* = 10.1 Hz), 133.45, 130.98, 130.69, 130.49 (d, *J* = 13.1 Hz), 127.46, 126.48, 124.10, 118.24 (d, *J* = 85.9 Hz), 67.98, 33.50, 29.50 (d, *J* = 17.2 Hz), 23.89, 22.86, 22.36; MS (ESI): *m/z*, 684.1 [M-Br]⁺; HRMS (ESI): calcd. for C₃₈H₃₃Cl₂NO₅P [M-Br]⁺: 684.1468, found: 684.1463.

4.2. Biological evaluations

4.2.1 Cell cultures

Cancer cell lines NCI-H1650, A375, and MCF-7, and the non-cancerous BEAS-2B cell line were purchased from Shanghai cell bank of Chinese Academy of Sciences (Shanghai, China). Cells were cultured in DMEM medium supplemented with 10% FBS, 1% penicillin and streptomycin. Cells grown at exponential stage were used for all the biological experiments.

4.2.2 Cell viability assay

Cell viability upon the treatment of the prepared compounds and DAP was tested by using the MTT assay. A suspension of cells (5000/well for NCI-H1650, 3500/well for MCF-7 and A375, and 4000/well for BEAS-2B) were seeded in 96-well plates and cultured for 24 h. Then seven different concentrations of **1a-f** ranging from 10-0.16 μM (PBS buffer containing 1% DMSO) and DAP (40-0.63 μM) were added into the 96-well plates, in which cells were incubated for 72 h. Then, 10 μL of MTT (0.5 mg/mL) solution was added to each well of the plates. After 4 h incubation at 37 $^{\circ}\text{C}$, the supernatant was removed and 100 μL DMSO was added, with the aid of gentle shaking to dissolve the formazan crystals in the plates. The absorbance of the each well was measured at 570 nm in a microplate reader (Bio-Rad Laboratories, Shanghai, USA). At last, resultant $\text{OD}_{570\text{ nm}}$ values were expressed as IC_{50} values, which were the mean values derived from three independent experiments.

4.2.3 Cell apoptosis detection

NCI-H1650 cells were seeded at a density of 4×10^5 cells/mL on each well of 6-well plates and were allowed to grow overnight. Then cells were treated with DAP (10 μM) and **1f** (0.5, 1, and 2 μM) for 12 h, and **1f** at 1 μM for 6, 12, 24 h. Cells were trypsinized, repeatedly washed with cold PBS for three times, centrifuged at 1200 rpm / min for 5 min, and the supernatants were discarded. Then cells were resuspended in $1 \times$ Annexin binding buffer to $\sim 5 \times 10^5$ cells/mL. To the 100 μL of cell suspension, 5 μL of Annexin V and 10 μL of PI were added and incubated for 15 min at room temperature. After the incubation, 400 μL of binding buffer was added to each sample and was gently mixed and analyzed immediately on a flow cytometer (Accuri C6, BD Biosciences).

4.2.4 JC-1 assay for flow cytometry analysis

NCI-H1650 cells were cultured on 6-well plates at a density of 4×10^5 cells/mL and allowed to grow overnight at 37 $^{\circ}\text{C}$. Cells were treated with **1b** (5 μM) and **1f** (1, 2, and 5 μM) for 4 h at 37 $^{\circ}\text{C}$. A solution of 1 μM JC-1 reagent in fresh medium was added and incubated at 37 $^{\circ}\text{C}$ for 15 min. Then the culture medium was removed. The cells were washed 3 times with cool PBS and trypsinized for 5 min at 37 $^{\circ}\text{C}$. The cells were isolated and washed 3 times in PBS and centrifuged (1000 rpm / min for 5 min). The

resulting cell pellet was resuspended in 100 μ L PBS and analyzed by BD FACSCalibur flow cytometry.

4.2.5 ROS measurement

NCI-H1650 cells were seeded at a density of 4×10^4 cells/mL on a dark, clear bottom 96-well plates and were allowed to grow overnight. Then culture medium was removed and a diluted DCFH-DA (Beyotime, Jiangsu, China) solution was added (100 μ L/well) to incubate the cells for 45 min at 37 °C. Remove the medium and washed with $1 \times$ PBS for three times. Then the cells were treated with **1b** (5 μ M), and **1f** (1, 2, and 5 μ M) at 37 °C for 4 h. At last, the plate was measured on a microplate reader at Ex / Em = 485 / 535 nm.

4.2.6 Western blotting assay

NCI-H1650 cells were seeded in 6-well plates and treated with compounds at desired concentrations for 12 h. Then the treated cells were incubated with cell lysate buffer for 15 min, and centrifuged at 12000 rpm / min at 4 °C for 15 min. Protein concentration for each sample was assessed by Pierce's BCA Protein Assay Kit and balanced to the same level, followed by a 8 min protein denaturation with SDS loading buffer at 100 °C. Proteins in the samples were separated by SDS-PAGE electrophoresis, transferred onto nitrocellulose filter membrane, blocked in 5% fat free milk for 2 h, probed with desired primary antibodies overnight, followed with secondary HRP-conjugated anti-rabbit IgG for 2 h. Membranes were finally scanned in a ChemiDoc MP Imaging System (Bio-Rad) after 2 min incubation in Clarity Western ECLSubstrate (Bio-Rad).

4.2.7 Statistical analysis

Data was reported as Mean \pm SD. Statistical analysis was performed using GraphPad Prism version 6.0 for Windows. * $p < 0.05$ was considered as statistically significant.

Acknowledgments

We thank the financial support from Chongqing University of the Start-up Research Grant (No: 0247001104409), and the National Natural Science Foundation of China (No. 21572027).

References

- [1] D. Hanahan, R.A. Weinberg, Hallmarks of cancer: the next generation, *Cell* 144 (2011) 646–674.
- [2] S.L. Zhang, Y. He, K.Y. Tam, Targeting cancer metabolism to develop human lactate dehydrogenase (hLDH)5 inhibitors, *Drug Discov. Today* (2018) <https://doi.org/10.1016/j.drudis.2018.05.014>.
- [3] M.G.V. Heiden, L.C. Cantley, C.B. Thompson, Understanding the Warburg effect: the metabolic

- requirements of cell proliferation, *Science* 324 (2009) 1029–1033.
- [4] M.G.V. Heiden, Targeting cancer metabolism: a therapeutic window opens, *Nat. Rev. Drug Discovery* 10 (2012) 671–684.
- [5] M.S. Patel, L.G. Korotchkina, Regulation of the pyruvate dehydrogenase complex, *Biochem. Soc. Trans.* 34 (2006) 217–222.
- [6] X.K. Yu, Y. Hiromasa, H. Tsen, J.K. Stoops, T.E. Roche, Z.H. Zhou, Structures of the human pyruvate dehydrogenase complex cores: a highly conserved catalytic center with flexible N-terminal domains, *Structure* 16 (2008) 104–114.
- [7] S.L. Zhang, X.H. Hu, W. Zhang, H.K. Yao, K.Y. Tam, Development of pyruvate dehydrogenase kinase inhibitors in medicinal chemistry with particular emphasis as anticancer agents, *Drug Discov. Today* 20 (2015) 1112–1119.
- [8] W. Zhang, S.L. Zhang, X.H. Hu, K.Y. Tam, Targeting tumor metabolism for cancer treatment: is pyruvate dehydrogenase kinases (PDKs) a viable anticancer target? *Int. J. Biol. Sci.* 11 (2015) 1390–1400.
- [9] S.M. Wigfield, S.C. Winter, A. Giatromanolaki, J. Taylor, M.L. Koukourakis, A.L. Harris, PDK-1 regulates lactate production in hypoxia and is associated with poor prognosis in head and neck squamous cancer, *Br. J. Cancer* 98 (2008) 1975–1984.
- [10] H. Hur, Y. Xuan, Y.B. Kim, G. Lee, W. Shim, J. Yun, I.H. Ham, S.U. Han, Expression of pyruvate dehydrogenase kinase-1 in gastric cancer as a potential therapeutic target, *Int. J. Oncol.* 42 (2013) 44–54.
- [11] M.I. Koukourakis, A. Giatromanolaki, G. Bougioukas, E. Sivridis, Lung cancer: a comparative study of metabolism related protein expression in cancer cells and tumor associated stroma, *Cancer Biol. Ther.* 6 (2007) 1476–1479.
- [12] M.I. Koukourakis, A. Giatromanolaki, E. Sivridis, K.C. Gatter, A.L. Harris, Pyruvate dehydrogenase and pyruvate dehydrogenase kinase expression in non-small cell lung cancer and tumor-associated stroma, *Neoplasia* 7 (2005) 1–6.
- [13] S. Kamarajugadda, L. Stemboroski, Q. Cai, N.E. Simpson, S. Nayak, M. Tan, J. Lu, Glucose oxidation modulates anoikis and tumor metastasis, *Mol. Cell. Biol.* 32 (2012) 1893–1907.
- [14] T. Hitosugi, J. Fan, T.W. Chung, K. Lythgoe, X. Wang, J. Xie, Q. Ge, T.L. Gu, R.D. Polakiewicz, J.L. Roesel, G.Z. Chen, T.J. Boggon, S. Lonial, H. Fu, F.R. Khuri, S. Kang, J. Chen, Tyrosine phosphorylation of mitochondrial pyruvate dehydrogenase kinase 1 is important for cancer metabolism, *Mol. Cell* 44 (2011) 864–877.
- [15] E. Saunier, C. Benelli, S. Bortoli, The pyruvate dehydrogenase complex in cancer: an old metabolic

- gatekeeper regulated by new pathways and pharmacological agents, *Int. J. Cancer* 138 (2016) 809–817.
- [16] T. Meng, D.D. Zhang, Z.Q. Xie, T. Yu, S.C. Wu, L. Wyder, U. Regenass, K. Hilpert, M. Huang, M.Y. Geng, J.K. Shen, Discovery and optimization of 4,5-diarylisoxazoles as potent dual inhibitors of pyruvate dehydrogenase kinase and heat shock protein 90, *J. Med. Chem.* 57 (2014) 9832–9843.
- [17] W.Y. Sun, Z.Q. Xie, Y.F. Liu, D. Zhao, Z.X. Wu, D.D. Zhang, H. Lv, S. Tang, N. Jin, H.L. Jiang, M.J. Tan, J. Ding, C. Luo, J. Li, M. Huang, M.Y. Geng, JX06 Selectively inhibits pyruvate dehydrogenase kinase PDK1 by a covalent cysteine modification, *Cancer Res.* 75 (2015) 4923–4936.
- [18] Y.F. Liu, Z.Q. Xie, D. Zhao, J. Zhu, F. Mao, S. Tang, H. Xu, C. Luo, M.Y. Geng, M. Huang, J. Li, Development of the first generation of disulfide-based subtype-selective and potent covalent pyruvate dehydrogenase kinase 1 (PDK1) inhibitors, *J. Med. Chem.* 60 (2017) 2227–2244.
- [19] J. Espinal, T. Leesnitzer, A. Hassman, M. Beggs, J. Cobb, Inhibition of pyruvate dehydrogenase kinase by halogenated acetophenones, *Drug Develop. Res.* 35 (1995) 130–135.
- [20] L.J. Qin, Y. Tian, Z.L. Yu, D.B. Shi, J.S. Wang, C.L. Zhang, R.Y. Peng, X.Z. Chen, C.C. Liu, Y.M. Chen, W.L. Huang, W.G. Deng, Targeting PDK1 with dichloroacetophenone to inhibit acute myeloid leukemia (AML) cell growth, *Oncotarget* 7 (2016) 1395–1407.
- [21] S.L. Zhang, X.H. Hu, W. Zhang, K.Y. Tam, Unexpected discovery of dichloroacetate derived adenosine triphosphate competitors targeting pyruvate dehydrogenase kinase to inhibit cancer proliferation, *J. Med. Chem.* 59 (2016) 3562–3568.
- [22] S.L. Zhang, W. Zhang, Q.P. Xiao, Z. Yang, X.H. Hu, Z.Y. Wei, K.Y. Tam, Development of dichloroacetamide pyrimidines as pyruvate dehydrogenase kinase inhibitors to reduce cancer cell growth: synthesis and biological evaluation, *RSC Adv.* 6 (2016) 78762–78767.
- [23] D.C. Wallace, Mitochondria and cancer, *Nat. Rev. Cancer* 12 (2012) 685–698.
- [24] J.A. Jara, V. Castro-Castillo, J. Saavedra-Olavarria, L. Peredo, M. Pavanni, F. Jana, M.E. Letelier, E. Parra, M.I. Becker, A. Morello, U. Kemmerling, J.D. Maya, J. Ferreira, Antiproliferative and uncoupling effects of delocalized, lipophilic, cationic gallic acid derivatives on cancer cell lines. Validation in vivo in syngenic mice, *J. Med. Chem.* 57 (2014) 2440–2454.
- [25] M. Eleni, Ladopoulou, A.N. Matralis, A. Nikitakis, A.P. Kourounakis, Antihyperlipidemic morpholine derivatives with antioxidant activity: an investigation of the aromatic substitution, *Bioorg. Med. Chem.* 23 (2015) 7015–7023.
- [26] E. Momán, D. Nicoletti, A. Mouriño, Synthesis of novel analogues of 1 α ,25-dihydroxyvitamin D3 with side chains at C-18, *J. Org. Chem.* 69 (2004) 4615–4625.

- [27] V. Cuchelkar, P. Kopečková, J. Kopeček, Novel HPMA copolymer-bound constructs for combined tumor and mitochondrial targeting, *Mol. Pharmaceutics* 5 (2008) 776–786.

ACCEPTED MANUSCRIPT

Highlights

- ▶ Target compounds have less side effect and more specific as compared with their parent molecule
- ▶ **1f** displayed a very strong PDKs inhibitory activity with an EC₅₀ value of 0.1 μM
- ▶ **1f** showed very promising cytotoxicity to cancer cells but little effect to normal cells